Geoderma 375 (2020) 114525

Contents lists available at ScienceDirect

Geoderma

journal homepage: www.elsevier.com/locate/geoderma

Using electromagnetic induction technology to identify atrazine leaching potential at field scale

Luciano Alves de Oliveira[a,*], Bryan L. Woodbury[b], Jarbas Honorio de Miranda[a], Bobbi S. Stromer[b]

[a] Department of Biosystems Engineering, "Luiz de Queiroz" College of Agriculture (ESALQ/USP), Av. Pádua Dias n.11 LEB/ESALQ/USP, 13.418-900 Piracicaba, SP Brazil
[b] USDA-ARS, U.S. Meat Animal Research Center, P.O. BOX 166, 68933 Clay Center, NE, United States

ARTICLE INFO

Handling Editor: Yvan Capowiez

Keywords:
Computational modeling
Water soil engineering
Soil solutes dynamics
Environmental contamination modeling
Soil herbicide dynamics

ABSTRACT

Atrazine is an herbicide commonly used to control weeds in corn crop. Atrazine becomes an environmental concern when it moves off-site to surface and ground waters. Understanding how atrazine moves in the field is important for developing management controls. Electromagnetic induction (EMI) has been used to map certain contaminant transport at the field scale. This study was developed to evaluate the efficacy of EMI technology for identifying surface soil atrazine concentration in a corn crop field. The research was conducted in a corn silage field with silt, clay and loam soils at the U.S. Meat Animal Research Center (USMARC), Clay Center, NE – USA, and it was divided in three stages; i) EMI data collection and a response surface sampling design for collection of bulk soils and soil core samples, ii) atrazine transport parameters were obtained by Breakthrough Curves using the bulk soil and numerical adjustments using STANMOD (HYDRUS package), and iii) Modeling atrazine parameters through EMI signal data with posterior atrazine's movement simulations through the soil using HYDRUS 2D. Atrazine's retardation factor, partition coefficient, and transfer coefficient were strongly correlated with EMI signal exhibiting a strong correlation with apparent electrical conductivity (EC_a). The low values for RMSE and RRMSE and the high values for Willmott and Pearson coefficients indicate EMI technology can be used to predict atrazine movement parameters. HYDRUS 2D quantitatively simulates the atrazine concentration leaching and how the temporal scale of this contamination would be. Combining EMI technology with HYDRUS 2D modeling provides researcher with additional information for developing better management practices for controlling atrazine movement to surface water; however, further studies are needed determine the effectiveness of this approach for other soil types.

1. Introduction

A growing challenge facing many countries is meeting the demand for food to feed a growing population. Endemic with this increase in food production is the expectation to minimize the environmental impact (Pittelkow et al., 2015). Herbicides are commonly used to control weeds and improve crop production around the world (Kniss, 2017). While herbicides are a powerful tool for weed control, these herbicides can become an environmental contaminant when they are transported off-site to surface and ground waters.

Atrazine (2-chloride-4-ethylamino-6-isopropylamino-striazine) is an herbicide commonly used to control weeds during corn production (NALEWAJA, 1968). Atrazine's mode of action for weed control is stopping CO_2 fixation thereby ceasing carbohydrate production (Taiz et al., 2013). Atrazine is also classified as toxic agent which disrupts the hormonal balance (Friedmann, 2002), and a type C carcinoma agent, which are potentially carcinogenic to humans (Biradar & Rayburn, 1995). It has been widely used throughout the world such as China (Yue et al, 2017), India (Saha, 2017), Brazil (Fernandes et al, 2020), and including the US (Hansen et al, 2019), although it was prohibited in Europe Union due to it contaminating groundwater in 2003 (Sass & Colangelo, 2006; Prado et al., 2014; Ackerman, 2007). Its application depends on the clay amount in the soil; however, it is reported to be applied at average rates of 240 mg L^{-1} (de Oliveira et al, 2019). Atrazine can present decay rates to 50% of its mass from 10 to 200 days (Yale et al, 2017) producing desethylatrazine and deisopropylatrazine, together with the hydroxylated degradation products, which are considered major degradation products (Rubira et al, 2020). Wang (2009) reported the clay fraction was the most important for atrazine retention due to the microporous structure. Work by Dor et al. (2019) also

* Corresponding author.
E-mail addresses: lucianooliveira21@hotmail.com (L.A. de Oliveira), bryan.woodbury@ars.usda.gov (B.L. Woodbury), jhmirand@usp.br (J.H. de Miranda), Bobbi.S.Stromer@usace.army.mil (B.S. Stromer).

https://doi.org/10.1016/j.geoderma.2020.114525
Received 28 January 2020; Received in revised form 2 June 2020; Accepted 5 June 2020

reported atrazine is trapped within the clay aggregates. They suggested disaggregation of this bound soil-atrazine matrix resulted in pesticide mobility and concluded stabilization of a sandy clay loam aggregates reduced atrazine leaching. They also reported that wetting and drying directly affects the soil microstructure, which can increase atrazine mobility.

One method for increase crop productivity while minimizing inputs is the use of precision agriculture (Anlauf et al.,2018). Precision agriculture attempts to use the specific types and amounts of production inputs for a given soil type. This is accomplished by increasing the number of correct decisions per unit area of land per unit time with associated net benefits (McBratney et al., 2005). Development and application of sensor data to improve information concerning each land unit is essential for precision agriculture to work effectively. One sensor that has been used effectively for identifying soil properties is electromagnetic induction (EMI) (Doolittle & Brevik, 2014).

Several studies have reported methodologies for using EMI to predict the spatial variability of soils. These studies use soil properties such as salinity, subsurface water movement and soluble salts, soil water content, soil texture, clay content, lithology and mineralogy, soil compaction, CEC, soil pH, and minerals to indicate changes (Cockx et al., 2009; Triantafilis et al., 2009; Sudduth et al., 2010; Al-Gaadi, 2012; Heil and Schmidhalter, 2012; Doolittle et al., 2013). Jaynes et al (1995) used EC_a measured by EMI as a surrogate measure of soil-herbicide partitioning. They found that using EC_a to map the soil adsorption coefficient (Kd) is rapid, easy, and inexpensive once it has been calibrated. However, EC_a failed to predict the observed high sorption coefficient values (K_d). Von Hebel et al (2018) combined depth-specific soil information obtained from the quantitative inversion of ground--based multicoil electromagnetic induction data with the airborne hyperspectral vegetation mapping. They found that soil structures at specific depths were identified by quantitative electromagnetic induction data inversions and confirmed by their soil samples. Whereas the upper plowing layer showed minor correlation to the plant data, the deeper subsoil carrying vital plant resources correlated substantially. Brogi et al (2019) used a multi-configuration of EMI survey combined to a supervised classification methodology to obtain a high-resolution map with detailed and quantitative representation of horizontal and vertical variability of soil properties. They found that a high-resolution map obtained through the EMI and ground-truth data was useful for defining that requires variable management within precision agriculture applications. Kaufmann et al (2020) aimed to evaluate the single and combined effects of irrigation and mineral and organic fertilizer applications on ECa obtained my EMI. They found that their experiment site indicated irrigation and fertilize management exhibited a legacy effect on ECa measures by EMI, offering new potentials in detecting and understanding effects of agricultural management on spatial soil properties at farm level.

Traditional methods for using covariate information to estimate spatial distribution of specific constituents use techniques such as kriging (Isaaks & Srivastava, 1989) or kriging with external drift (Wackernagel, 1998). These techniques can be effective but usually require many samples to get adequate estimates on key statistical parameters. An alternative to these methods, using multilinear regression, has been used extensively for describing salt-affected irrigated soils and it is response surface sampling design (RSSD) (Corwin and Lesch, 2005; Rhoades et al., 1999; Lesch et al., 1995a,b).

Previous studies (Woodbury et al., 2011; Eigenberg et al., 2008; Lesch, 2005) have shown that RSSD, coupled with correlation analysis and multilinear regression has resulted in predictive maps of contaminants at the field scale. In addition, this process has been effectively combined with time-lapse analysis to visually illustrate control points or the impact of mitigation control practices. RSSD also has the advantage of using EC_a as a co-variant allowing for fewer calibration soil samples to be taken to provide insight to field scale spatial dynamic.

Modeling is another tool that collaborates with the precision agriculture development (Dourado Neto et al., 1998). HYDRUS is a software package, which includes several models of water and solute movement through the soil. It uses boundaries conditions to numerically predict soil conditions. Studies have documented the efficacy of HYDRUS (de Oliveira et al, 2019; Šimůnek and Hopmans, 2009) attesting that it is widely used in many industrial and environmental applications, as well as for addressing many agricultural problems (Šimůnek et al., 2016). Examples of existing agricultural applications include irrigation management (Bristow et al., 2002; Dabach et al., 2015), drip and sprinkler irrigation design (Bristow et al., 2002; Gärdeñas et al., 2005; Hanson et al., 2008; Kandelous et al., 2012), studies of root water and nutrient uptake (Šimůnek and Hopmans, 2009; Vrugt et al., 2001a,b), and solutes movement through the soil (de Oliveira et. al, 2019; Grecco et al., 2019; Matteau et al., 2019).

With all the concerns regarding atrazine contamination, using EMI to identify areas of a field that are more susceptible for atrazine to move off-site and coupling with a hydrological model like HYDRUS will allow producers to implement management practices to mitigate this risk. Several authors (Gish et. al, 1991; Sadeghi et. al, 1995; Close et. al, 1998; Mao et. al, 2005; Deng et. al, 2017) have studied atrazine movement parameters such as its partition coefficient (β), and mass transfer coefficient (ω). These parameters present values that range from 0.3 to 0.9 for β and 0.5 to 20 h^{-1} for ω (de Oliveira et. al, 2019). However, only Jaynes et al (1995) have tried to correlate K_d with EMI. Therefore, it is necessary to make a deep assessment about this correlation that will be useful for researchers to better understand the complex transport process at the field scale and handle atrazine and policy makers to make decisions regarding environmental regulatory requirements.

Therefore, the overall objectives of this study were to determine whether EMI can be used to identify regions at the field scale to mitigate atrazine transport to groundwater by understanding how atrazine moves at field-scale, identifying surface soil atrazine concentration, and predict atrazine movement through the soil. Specific objectives were to i) use response surface sampling design (RSSD) to identify spatially variable atrazine transport parameters of a corn silage field; ii) measure breakthrough curves of the soil identified using RSSD and determine whether EMI can adequately predict the spatial variable atrazine's transport, iii) use these predicted transport parameters as inputs to the HYDRUS 2D to estimate atrazine loss to groundwater through the soil profile and iv) evaluate the effectiveness of HYDRUS 2D for spatial accuracy.

2. Material and methods

2.1. Experiment summary

The demonstration site was selected to evaluate transport through the soil profile which could result in groundwater contamination as well it is understood atrazine application to an area subject to erosion could contaminate surface waters. The application of EMI technology for identifying the risk for surface water contamination will be the subject of future studies. The site selected was a 68- by 133 m corn silage field at the U.S. Meat Animal Research Center (USMARC) (Fig. 1B), Clay Center, NE - USA, with D_{FA} climate (Hot summer continental climate) according to the Köppen classification (40° 31′ 20″ N, 98° 3′ 18″ W, and 529 m of altitude) (Fig. 1A). The site transected includes a transition between two soil types resulting from topographical relief. The soil in the area is classified as a Hastings silt loam complex, however, four different textures were found in the area (Table 1), and the retention curve (Eq. (1)) for the major component was considered (Fig. 2).

The soil retention curve was described using the standard equations of van Genuchten (1980):

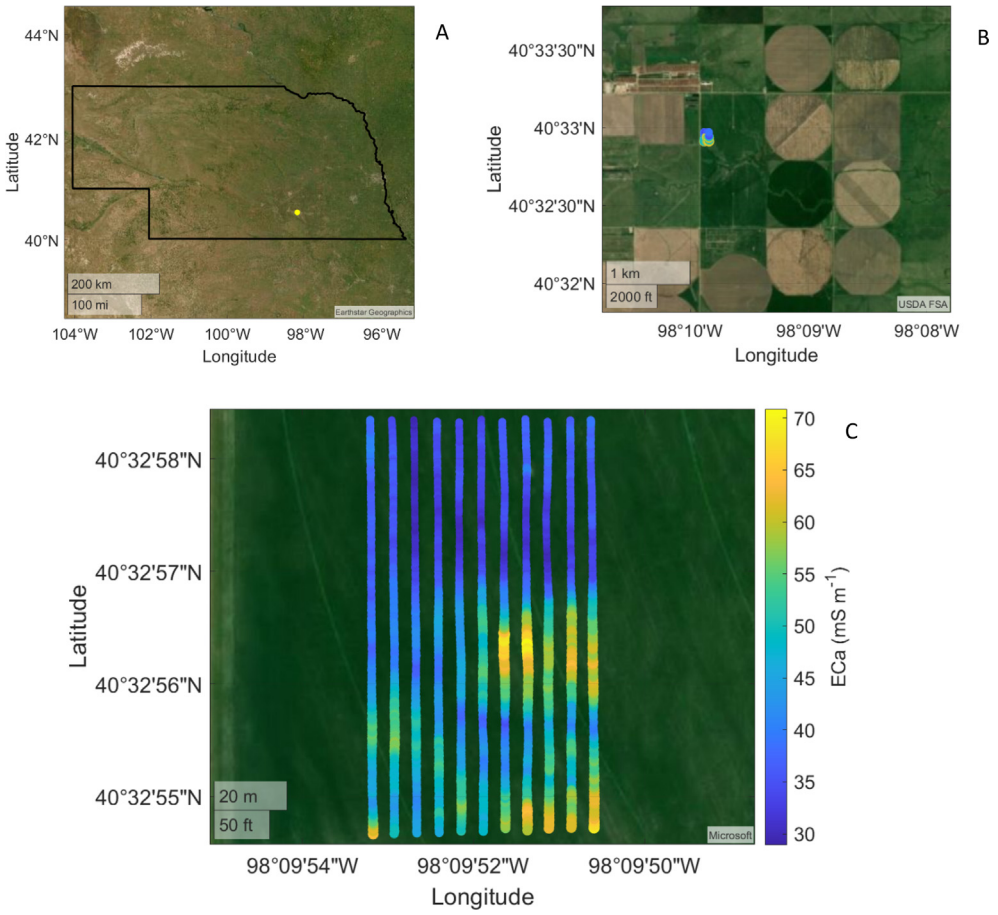

Fig. 1. (A) Nebraska State and Clay Center location (yellow dot represents the city). (B) Location of corn silage field in the USMARC at Clay Center/NE (blue dot represent the group of data collected). (C) Electromagnetic Induction (EMI) survey data of the corn silage field. Output is apparent electrical conductivity (ECa). The markers are the twelve locations selected by response surface sampling design (RSSD) where samples were collected.

Table 1
Physical properties of the different soils in the corn silage field.

Properties	SOIL 1	Soil 2	Soil 3	Soil 4
Texture Class	Silt Loam	Clay Loam	Silty Clay Loam	Clay
Sand (%)	24	22	18	21
Silt (%)	51	43	49	33
Clay (%)	25	35	33	46
Field capacity ($cm^3\ cm^{-3}$)	0.30	0.27	0.31	0.32
Wilting point ($cm^3\ cm^{-3}$)	0.10	0.12	0.12	0.16
Bulk density ($g\ cm^{-3}$)	1.3	1.3	1.3	1.3
Organic Matter (%)	4.4	4.2	3.7	3.9
Saturated Hydraulic Condctivity - K_s ($cm\ h^{-1}$)	0.48	0.50	0.51	0.49

$$\theta(\varphi_m) = \theta_r + \frac{\theta_s - \theta_r}{[1 + (\alpha\ |\varphi_m|)^n]^m} \quad (1)$$

$$K(h) = K_s S_e^l [1 - (1 - S_e^{1/m})^n]^2 \quad (2)$$

where θ (φ_m) is the water content in a given tension, θ_r and θ_s are the residual and saturated soil water contents (L^3L^{-3}) respectively, φ_m is tension (L), α (L^{-1}), n and m (–) are dimensionless shape parameter of the soil water retention curve, with m = 1–1/n, and S_e is effective saturation given by:

$$S_e = \frac{\theta - \theta_r}{\theta_s - \theta_r} \quad (3)$$

The research was conducted in three distinct stages. First EMI was used to collect EC_a data from the plot. This EC_a data was used to generate a response surface sampling design (RSSD) that selected 12 sampling sites to represent the spatial variability of the plot (Fig. 1B).

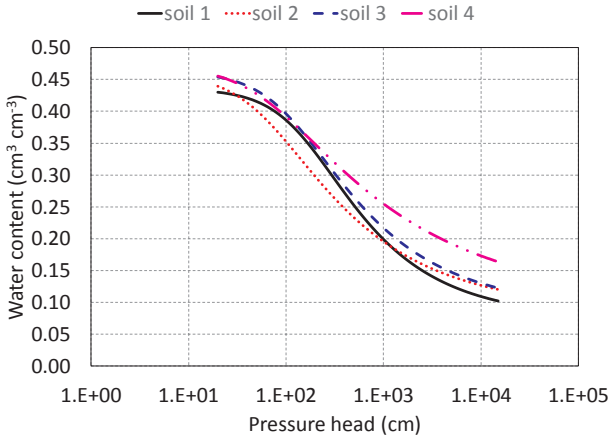

Fig. 2. soil water retention curve of the soils at the corn silage field.

The GPS coordinates for the EC_a data were used to navigate to the 12 sampling sites to collect bulk soil to a depth of 40 cm (Fig. 1B). Next, breakthrough curves for each site were determined for each sampling site. These data were used to determine transport parameters using STANMOD (HYDRUS package). Finally, these transport parameters were correlated with the EC_a data to determine whether EMI was an effective tool for predicting atrazine's movement through soil.

2.2. Corn crop survey

The corn crop was planted on 30 May 2018 and atrazine (5.7 L ha^{-1} Volley atrazine NXT) was applied post emergence on 12 Jun 2018. Prior to planting, the spatial EC_a data were collected from the site using

methods detailed in Woodburry et al. (2009). A brief description follows: a DualEM-1S meter (DualEM Inc., Milton, ON, Canada) was used to collect EC_a data from the corn field surface. The instrument was calibrated at the Corn field for phasing and zeroing using the manufacturer's standard calibration method after a warm-up period of 1 h. The meter was positioned on a nonmetallic sled and pulled with an all-terrain vehicle (ATV) at approximately 1.5 m s^{-1} at 6 m intervals across the corn field. Path spacing was maintained using a Trimble EZ – Guide Global Positioning System (GPS) – Guidance System (Trimble Navigation LTD, Sunnyvale, CA) which was mounted on the ATV. The DualEM-1S meter simultaneously records both horizontal and vertical dipole modes; however, only the vertical orientation was used for this study (centroid response depth-measure approximately 0.5 m). Simultaneously, GPS coordinates of the instrument's position were determined using an AgGPS 332 receiver using real-time kinematic (RTK) correction (Trimble Navigation Ltd). Coordinates and EC_a data were collected at a rate of five samples per second and stored in a Juniper System Allegro (Juniper Systems, Logan, UT) datalogger. Edge effects from metal fencing were clipped from the EC_a data set using ESAP-RSSD (Lesch et al., 2000) before the sampling designs were determined.

Response Surface Sampling Design (RSSD) is a software program contained in the USDA-ARS EC_e Sampling, Assessment and Prediction (ESAP) software package (Lesch et al., 2000) and it was used to select 12 sites in the corn field. The GPS coordinates associated with the selected EC_a values were used to navigate back to these sites for collecting bulk surface soil. The RSSD algorithm (Lesch, 2005) selects more samples near the extremes of the signal data distribution, resulting in larger observed variance response variables (if and when the response variable[s] are sufficiently correlated with the EMI survey data).

ESAP software package contains a sampling approach specifically designed for use with ground-based EC_a signal readings (Lesch, 2005), based on the observed magnitudes and spatial locations of the EC_a data, a minimum set of calibration samples were selected. These sites were chosen in an iterative, nonrandom manner to optimize the estimation of a regression model, and simultaneously maximize the average separation distance between adjacent sampling locations. Lesch, (2005) demonstrated that such a sampling approach can substantially outperform a probability-based sampling strategy with respect to a number of important model-based prediction criteria.

2.3. Sample collection and analysis

Once the sampling designs were generated, bulk soil samples were collected to a depth of 40 cm at all 12 sites to run breakthrough curves (BTC's) for determining atrazine movement parameters: Retardation factor (R), partition coefficient (β) and transfer coefficient (ω). The soil was air dried and mechanically ground to pass through a 2-mm sieve.

The BTC analyzes were done to obtain laboratory atrazine transport parameters. The soil columns were saturated with $CaCl_2$ solution to prevent the clays from swelling, by capillarity, aiming to expel the air contained in micro pores. To accomplish this, the columns were placed in a bucket and water was added by dripping along the walls of the bucket until it reached about 2/3 of the height of the soil column. The columns remained in the bucket for 24 h to allow for complete saturation. After saturation, the columns were placed in an apparatus such to allow a constant head of $CaCl_2$ solution (3 mmol L^{-1}) to be maintained at the top of the soil column. To facilitate solute movement, an 80 kPa suction tension was applied at the bottom. The $CaCl_2$ was passed through the soil columns for 24 h to establish steady-state flow. Once steady-state flow was established, a two-pore volume atrazine pulse (5 mg L^{-1}) in the same $CaCl_2$ solution was passed through. Following the atrazine pulse, the $CaCl_2$ solution was reintroduced. Steady-state flow conditions were maintained throughout the study.

The concentration of Atrazine in each flask was determined using liquid–liquid extraction followed by analysis using Ultra Performance Liquid Chromatography (UPLC). Atrazine was separated from other soil leachates using a Waters BEH C18 column (50 mm, 2.1 mm × 1.7 μm) at 40 °C with an isocratic mobile phase of 1:1 (v/v) Methanol:Water and a flow rate of 0.2 mL min^{-1}. Concentrations were determined by measuring the atarazine abosrbance at 220 nm. Calibration curves were established prior to each analysis.

There were 5 sampling dates (31 May, 24 Jun, 30 Jul, 3 Aug, 30 Aug 2018) spread across the crop growing season. Soil samples were collected at the same RSSD sites described earlier. The samples were dried and ground to pass through a 2 mm sieve to prepare the samples for atrazine extraction. First, 10 g of the sample was separated into a 50 mL conical tube where 14 mL of 0.5 M aqueous Ammonium Nitrate and 6 mL of methanol were added. Samples were then shaken on a reciprocating shaker for 30 min at 150 rpm. The samples were centrifuged at 1500 rpm and the supernatant poured off into a secondary 120 mL container. This step was repeated 2 times and the supernatant from each step combined. Next, 20 mL of Acetone was added, the samples were shaken as before, and the supernatant collected and added to the supernatant from the previous two steps. The supernatant was collected in each step Methanol and Acetone were evaporated by flowing nitrogen over the samples for 50 min at 38° C. The sample was brought up to 100 mL using deionized water. The solution was passed through solid phase extraction cartridges (Waters Oasis, 6 cc 200 mg HLB) for atrazine extraction. Thus, atrazine was eluted off the cartridges using 3 mL of 0.5% Formic Acid in Methanol and the flow through collected in a test-tube. Nitrogen was used to reduce sample volume to approximately 100 μL before water was used to bring the sample volume back up to 1 mL. The solutions were filtered through 0.22 μm nylon syringe filter and analyzed for atrazine concentration using UPLC. Separation for atrazine was accomplished on a Waters BEH C18 column (50 mm, 2.1 mm × 1.7 μm) T 40 °C using an isocratic mobile phase of 1:1 (v/v) Methanol:Water and a flow rate of 0.2 mL min-1. Atrazine peak was monitored at 220 nm.

2.4. Atrazine transport

The STANMOD (Studio of ANalytical MODels) was the software chosen to determine atrazine's transport parameters. It presents adequate performance in numerical adjusts, broad variety in boundary conditions, free license, and has plenty of tutorials and technical support (Šimůnek et al., 1999). These parameters were numerically determined using one of the models in it called CXTFIT (TORIDE, et al. 1995) using equation (4a) and (4b). The model is used to estimate parameters in several analytical models for solute transport during steady one-dimensional flow by fitting the parameters to laboratory or field data observed, obtained from solute displacement experiments (Wang et al, 2020).

$$\beta R\frac{\partial C_1}{\partial T} + (1-\beta)R\frac{\partial C_2}{\partial T} = \frac{1}{P}\frac{\partial^2 C_1}{\partial x^2} - \frac{\partial C_1}{\partial x} \tag{4a}$$

$$(1-\beta)R\frac{\partial C_2}{\partial T} = \omega(C_1 - C_2) \tag{4b}$$

Where

$$\beta = \frac{\theta_m + \rho f_m K_D}{\theta + \rho K_D} \tag{5}$$

$$P = \frac{v_m L}{D_m} \tag{6}$$

$$R = 1 + \frac{\rho K_D}{\theta} \tag{7}$$

$$\omega = \frac{\alpha_m L}{q} \tag{8}$$

$$C_1 = \frac{C_m}{C_0} \tag{9}$$

$$C_2 = \frac{C_{im}}{C_0} \tag{10}$$

where: R is the retardation factor (dimensionless); C is the relative solute concentration (dimensionless); T is the relative time (dimensionless); P is the Peclet number (dimensionless); x is the relative distance (dimensionless); ρ is the bulk density (g cm^{-3}); θ is the volumetric soil–water content (cm^3 cm^{-3}); C_0 is initial concentration (μg L^{-1}); v is the average pore water velocity (cm h^{-1}); q is the Darcy flux (cm h^{-1}); L is the column length (cm); C_m and C_{im} are concentrations (μg L^{-1}) in the mobile and immobile regions, respectively; θ_m is the mobile water content (cm^3 cm^{-3}); f_m is the fraction of the soil in equilibrium with the mobile water (dimensionless); v_m is the pore water velocity (cm h^{-1}) in the mobile region; D_m is the mobile pore water hydrodynamic dispersion coefficient (cm^2 h^{-1}); α_m is the first order mass transfer coefficient (h^{-1}); β is the fraction of solute in the mobile region or partition coefficient (dimensioless); and ω is the mass transfer coefficient (h^{-1}).

2.5. Hydrus-2D simulations

To obtain HYDRUS-2D simulations, site environmental conditions were needed where the experiment is located. Thus, information from the soil, corn, atrazine application, irrigation management, geometry of the system, time unit and boundary conditions are explained as follows.

The sprinkler irrigation process was modeled using HYDRUS-2D (Šimůnek et al., 1999) based on the following form of the Richards equation for an isotropic soil profile:

$$\frac{\delta\theta(h)}{\delta t} = \frac{\delta}{\delta x}\left(K(h)\frac{\delta h}{\delta x}\right) + \frac{\partial K(h)}{\partial x} - s(h) \tag{11}$$

where θ is the volume water content in the soil ($L^3.L^{-3}$); h is the water head (L); K is the soil hydraulic conductivity ($L.T^{-1}$); t is time (T); s is root water uptake (T^{-1}) as described with the uptake model by Feddes et al. (1978):

$$S(h) = \gamma(h)\zeta(r, z)WT_p \tag{12}$$

where $\gamma(h)$ is the soil water stress response function (–); ζ is the normalized root water uptake distribution (L^{-2}); T_p is the potential transpiration rate (LT^{-1}); and W is the area of the soil surface (L^2) associated with the transpiration process.

In this study we used soil hydraulic parameters provided by the pedotransfer function present in HYDRUS-2D model through Rosetta.

HYDRUS models present a database for root water uptake for different plants based on Wesseling et al. (1991) and Taylor and Ashcroft (1972) and the corn was chosen. The spatial root distribution was described using the model of Vrugt et al. (2001a,b). The geographical positions were: latitude (40° N); altitude (529 m); Angstrom coefficients (a = 0.25 and b = 0.50) standard values.

The geometry information was chosen for two dimensions, unity in centimeters and the initial size was set as a rectangle with a width of 60 cm and a depth of 50 cm. This rectangle was discretized into 1959 two-dimensional elements involving 1035 nodes. Two observation nodes were included at 20 and 40 cm depth in the flow domain to follow simulated atrazine concentration versus time. The observation nodes had similar coordinates as the extractors installed in the containers to allow comparisons of observed and simulated data. It was also determined that the simulations were for water flux, solute transport and water and solute root uptake.

The time unit was days with minimum interval of 0.001 day for model operation. The output time unit was average by day. The hydraulic model used was van Genuchten-Mualem from van Genuchten (1980). The dual-porosity model with two-site sorption in the mobile zone (physical and chemical non-equilibrium) was chosen. The solute parameters and reactions parameters were set as obtained before.

A time-variable flux boundary condition was applied at the up part of the rectangle. During irrigation the sprinkler boundary was held at a constant flux. An atmospheric boundary condition was assumed for the entire soil surface. A no-flow boundary condition was established along the left and the right edges of the soil profile, and along part of the container's bottom. A drain was assumed at the container's bottom with the actual drainage being considered. The initial soil water content was the field capacity for each soil while the initial atrazine concentration was set as 0 μg cm^{-3}.

Potential evapotranspiration was calculated using the Penman-Monteith equation (Allen and Pereira, 1998) as implemented in the HYDRUS-1D software (Šimůnek et al., 1999). The simulations require daily estimates of potential evapotranspiration and transpiration.

2.6. Model specification, assumptions and evaluation

Hence, the following spatially referenced, multivariate linear regression (LR) model $y_{ij} = A + B(EMI_i) + \varepsilon_{ij}$ was used to describe the relationships between atrazine movement parameters (R, β and ω) and the EMI signal data; where y_{ij} is the value of the jth chemical property at the ith sampling location; A; B are the unknown regression model parameters for the jth regression equation (j = 1 and 2); and ε_{ij} is the jth spatially uncorrelated random normal error component.

A critical assumption is that the regression model errors are normally distributed and spatially uncorrelated. These assumptions must be verified before using an ordinary linear regression (OLR) model for prediction. The Moran residual test statistic (Tiefelsdorf, 2000) was used to assess the validity of the uncorrelated error assumption. Additionally, the normality assumption was assessed using Shapiro-Wilk test (Myers, 1986; Shapiro and Wilk, 1965).

The models which presented regression coefficients higher than 0.5 were statistically significant below the 0.05 significance level and considered adequate for predicting movement parameters for atrazine. Additionally, models with regression coefficients higher than 0.70 were considered adequate for mapping spatially referenced atrazine s movement parameters based on EC_a survey data. The indices Root Mean Square Error (RMSE), Willmot agreement index (d), and Pearson correlation coefficient (r) were used to evaluate the EMI model.

Maps with different interpolated data were generated using natural neighbor interpolation (Sibson, 1981) through MATLAB™ to spatialize the atrazine's movement parameters in the corn field. Then, a comparison between observed and simulated data was done using the indices previously described.

Lastly, maps using relative errors comparing the two different simulations scenarios to assess atrazine movement were created. The first scenario is using the average of all the atrazine movement parameters to simulate atrazine movement through the area. The second scenario is using the atrazine movement parameters obtained in each site and interpolating the results with the model (atrazine-soil properties) provided in this research. Two months were selected to make this comparison: July, after the atrazine application, and October, close to the harvest. The relative error was calculating as follows

$$R_e = \frac{[atz] - \bar{[atz]}}{[atz]} x100 \tag{20}$$

where, Re is relative error, %, $\bar{[atz]}$ is the atrazine concentration in average, and $[atz]$ is the atrazine concentration.

3. Results

The basic EC_a survey and atrazine parameters summary statistics are presented in Table 2. The shallow EC_a signal data exhibited an average of 43.0 mS m^{-1}, a standard deviation of 9.3 mS m^{-1}, and a range from 28.9 to 70.9 mS m^{-1}. A map of the acquired EC_a data for the sampling site are shown in Fig. 3 (along the sampling positions). The average retardation factor was 7.45 with a standard deviation of 4.35. The range of retardation factors was from 1.95 to 16.48. The average

Table 2
Basic EC_a data as measured by EMI and measured atrazine transport parameters summary statistics.

Variable	N	average	SD	Min	Max	SW (p-value)	S_M (p-value)
EC_a (mS m^{-1})	2496	43.0	9.3	28.9	70.9	–	–
Clay (%)	12	32.08	5.96	12.00	46.00	0.9196 (0.0845)	1.1426 (0.0934)
R	12	7.45	4.35	1.95	16.48	0.9468 (0.0677)	1.2400 (0.0871)
β	12	0.47	0.19	0.11	0.80	0.9529 (0.1291)	0.9246 (0.2120)
ω (h^{-1})	12	5.56	5.38	0.20	17.46	0.9493 (0.0520)	0.9647 (0.1459)

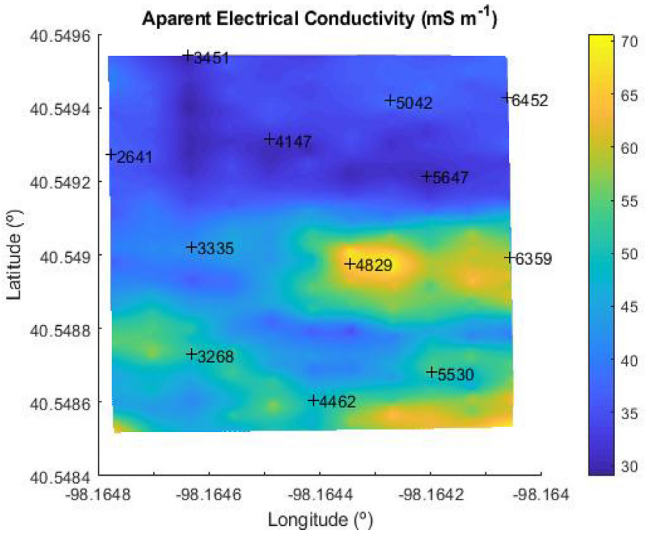

Fig. 3. EMI signal data spatialized along the sampling positions within the corn silage test site.

partition coefficient (β) was 0.47 with a standard deviation of 0.19. The range of β was from 0.11 to 0.80. Lastly, the average of transfer coefficient (ω) parameter was 5.56 h^{-1} with a standard deviation of 5.38 h^{-1}. The range of the ω parameter was 0.20 to 17.46 h^{-1}.

Before correlating soil properties with the EC_a in an OLR, it is necessary to analyze the assumptions about normality and spatial autocorrelation of the errors. Table 2 shows both Moran's test (S_m) and Shapiro-Wilk test (SW) that represent spatial autocorrelation and normality, respectively. For all the soil properties, clay, R, β and ω, the errors are considered normal and spatial uncorrelated. The S_M and SW values presented in Table 2 were not significant at the 0.05p-value for both indices' indicating the data are reasonably are normal and not spatial autocorrelated.

Fig. 4 presents the OLR between EC_a and the soil properties. Fig. 4A shows the regression line for clay content and the EC_a data. The R^2 is 0.8965 indicating good correlation between the two variables. Fig. 4B shows the model curve for retardation factor(R) and EC_a data. The R^2 is 0.9104 indicating strong positive correlation between EC_a and R. Fig. 4C shows the regression line between the parameter β and EC_a signal data. The R^2 is 0.8172 indicating good inverse correlation. Fig. 4D shows the model curve for parameter ω and the EC_a data. The R^2 is 0.9206 also indicating good correlation.

Fig. 4 also shows indices for modeling evaluation. The RMSE for clay, R, β and ω were 1.8453%, 1.2755, 0.0788, and 1.4821 h^{-1}, respectively. The r index for clay, R, β and ω was 0.9451, 0.9541, 0.9040, and 0.9595, respectively. And the d index was 0.9178, 0.9760, 0.9999, and 0.9815, respectively.

Fig. 5 presents the spatial distribution of atrazine-soil properties based on the co-variant soil EC_a. Fig. 5A illustrates the spatialized clay content (%) for the upper 40 cm of the sampling site. As the EC_a data decrease (Fig. 3), clay content (Fig. 5A), the retardation factor (Fig. 5B), and transfer coefficient (Fig. 5D) values also decrease. Contrary to this trend, is the parameter β (Fig. 5C). The values for β increase as the EC_a data decrease due to the inverse relation (see Fig. 4). The β factor is a measure of the proportion of the mobile water to immobile water. With increasing clay content, the immobile water proportion increases such β decreases. Also, the greater clay content of the surface soil increased the proportion of the immobile water to the mobile water thereby decreasing the β factor.

To evaluate atrazine's movement through the soil, simulations were taken along the time that the corn crop was in the field. Table 3 presents the indices of comparison between simulated and observed data. For RMSE at 20 cm depth, the lowest value was for the site 3268 with 0.0711 μg L^{-1} and the highest was the site 3451 with 0.3885 μg L^{-1}. The average error was 0.2079 μg L^{-1} while the standard deviation SD was 0.0984 μg L^{-1}. For 20–40 cm depth, the small RMSE value was for the site 6359 with 0.0526 μg L^{-1} and the highest value was for site 2641 with 0.3892 μg L^{-1}. The average error was 0.1476 μg L^{-1} and the SD was 0.0990 μg L^{-1}.

At 20 and 40 cm depths, Pearson coefficients were in between 0.8287 and 0.8998 indicating that the models are precise for obtaining atrazine movement parameters. For the same depths, Willmott agreement indices ranged between 0.8710 and 0.9923, indicating that the models are accurate for obtaining atrazine movement parameters.

Fig. 6 shows the atrazine concentration in July in three different conditions: simulation using the average of all the parameters sampled along the field at 20 and 40 cm depths (Fig. 6A and 6B, respectively); simulation using the site-specific parameters at 20 and 40 cm depths (Fig. 6C and 6D, respectively); and the relative error of average and site-specific parameters at 20 cm and 40 cm depths (Fig. 6E and 6F, respectively). When using the average of atrazine transport parameters, the field as whole presents 0.585 μg L^{-1} at 20 cm and 0.06 μg L^{-1} at 40 cm. In the other hand, when using the site-specific atrazine transport parameters, the field starts to present differences in the atrazine concentration at 20 cm. There are two different regions: one in the North part of the field where atrazine concentration is higher, reaching 2.5 μg L^{-1}, and one in the South part of the field where atrazine concentration is lower, being 0.25 μg L^{-1}. For 40 cm, atrazine concentrations have lower values varying from 0.04 to 0.06 μg L^{-1}. Comparing average and site-specific conditions, the relative errors vary from −56 to 331% for 20 cm, while for 40 cm the relative errors vary from −27 to 15%.

Fig. 7 shows the atrazine concentration in October in three different conditions: simulation using the average of all the parameters sampled along the field at 20 and 40 cm depths (Fig. 7A and 7B, respectively); simulation using the site-specific parameters at 20 and 40 cm depths (Fig. 7C and 7D, respectively); and the relative error of average and site-specific parameters at 20 cm and 40 cm depths (Fig. 7E and 7F, respectively). When using the average of atrazine transport parameters, the field as whole presents 0.015 μg L^{-1} at 20 cm and 0.29 μg L^{-1} at 40 cm depth. In the other hand, when using the site-specific atrazine transport parameters, the field starts to present differences in the atrazine concentration at 20 cm and 40 cm. There are two different regions: one in the North part of the field where atrazine concentration is lower, being close to 0.01 μg L^{-1}, and one in the South part of the field where atrazine concentration is higher, being 0.25 μg L^{-1}. For 40 cm, atrazine concentrations have higher values varying from 1.4 to 2.1 μg L^{-1}. Comparing average and site-specific conditions, the relative errors vary from −100 to 8500% for 20 cm, while for 40 cm the relative errors vary from 400 to 600%.

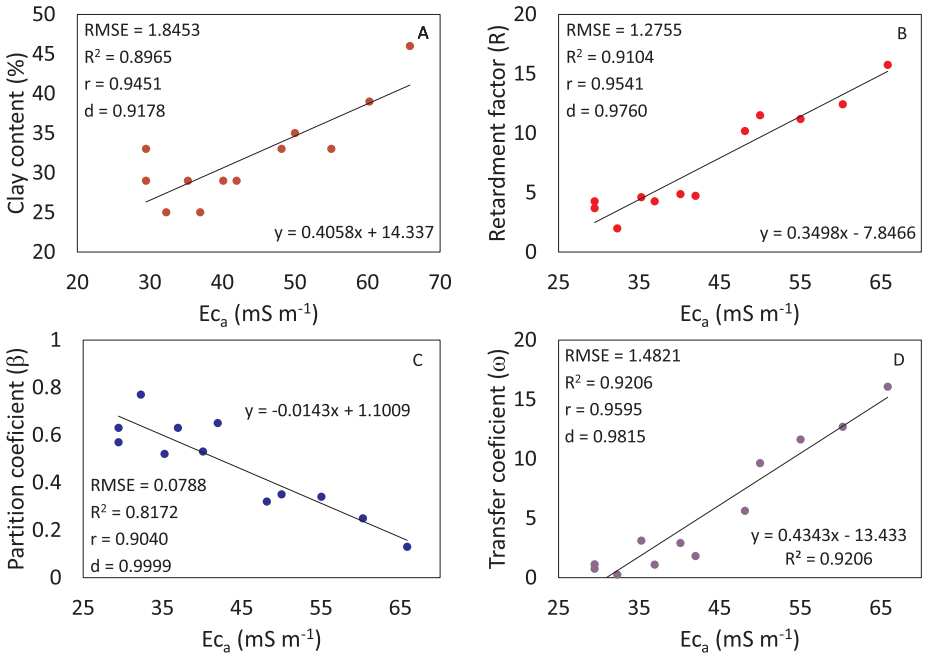

Fig. 4. Ordinary Linear model (Atrazine-Soil properties) to predict (A) clay content, %, (B) R - Retardation factor (–), (C) β - partition coeficiente (–), and (D) ω - transfer coefficient (h^{-1}).

4. Discussion

The excellent correlation found by this study between the shallow EMI signal data and the clay content, retardation factor, partition coefficient and transfer coefficient confirm that EMI survey data can be effectively used to map spatially variable atrazine transport parameters through the soil profile of a corn silage field. This suggest that this assessment methodology can be more broadly applicable specially when coupled with different technologies such as HYDRUS-2D. Each of the four linear regression models presented in Fig. 4 (clay, R, β and ω)

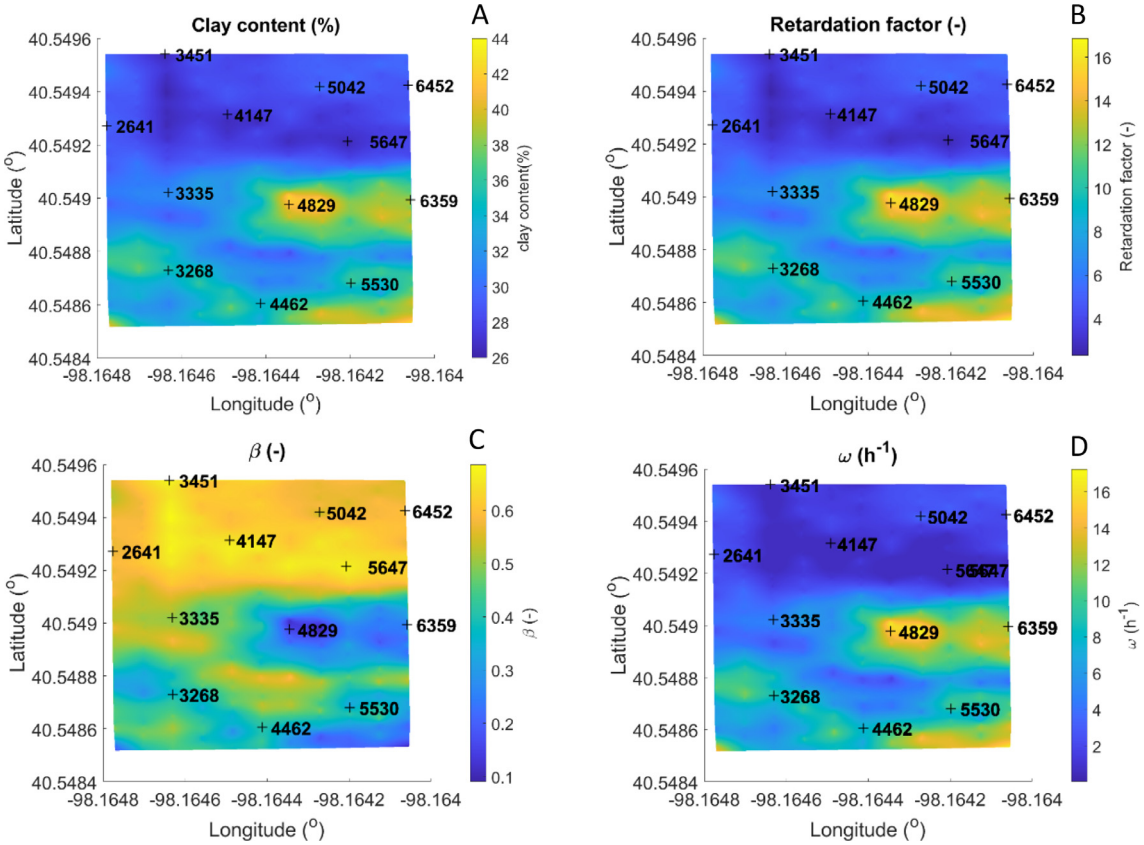

Fig. 5. Soil properties spatialized according to linear model (Atrazine-Soil properties). (A) clay content, %, (B) R - Retardation factor (–), (C) β - partition coeficiente (–), and (D) ω - transfer coefficient (h^{-1}).

Table 3
Atrazine movement parameters and Indices of comparison between observed and modeled data for each site. Root mean square error (RMSE), Pearson coefficient (r), Willmott agreement index (d), standard deviation (SD).

Site	Clay content (%)	R	β	ω (h^{-1})	RMSE (μg L^{-1})		r		d	
					20 cm	40 cm	20 cm	40 cm	20 cm	40 cm
2641	25	4.27	0.63	1.09	0.2030	0.3892	0.8757	0.9196	0.8529	0.8710
3268	35	11.50	0.35	9.63	0.0711	0.0912	0.8848	0.9891	0.8642	0.8899
3335	29	4.72	0.65	1.81	0.1199	0.1061	0.8894	0.9770	0.8353	0.8965
3451	29	4.26	0.57	1.13	0.3885	0.2291	0.8941	0.9200	0.8632	0.9442
4147	25	1.99	0.77	0.27	0.2863	0.1583	0.8921	0.9639	0.8789	0.9720
4462	33	10.17	0.32	5.62	0.1377	0.0825	0.8597	0.9479	0.8287	0.9529
4829	46	15.74	0.13	16.05	0.1164	0.0347	0.8221	0.9615	0.8751	0.8718
5042	29	4.87	0.53	2.92	0.3064	0.1441	0.8998	0.9597	0.8705	0.9733
5530	33	11.19	0.34	11.63	0.1467	0.0797	0.8991	0.9383	0.8395	0.9289
5647	33	3.68	0.63	0.75	0.3021	0.2259	0.8979	0.9767	0.8759	0.9485
6359	39	12.43	0.25	12.68	0.1553	0.0526	0.8965	0.9479	0.8597	0.9453
6452	29	4.60	0.52	3.1	0.2619	0.1779	0.8998	0.9923	0.8769	0.9563
average	32.08	7.45	0.47	5.56	0.2079	0.1476	0.8843	0.9578	0.8601	0.9292
SD	5.96	4.35	0.19	5.38	0.0984	0.0990	0.0229	0.0241	0.0174	0.0372

explained > 80% of the variation in these elements. The fitted regression models were, in fact, used to estimate the atrazine movement through the soil profile at the hand of HYDRUS-2D, which accurately simulated the spatial and time variation of atrazine concentration. The correlation between EMI signal data and atrazine transport parameters is driven by the clay type and content of the near-surface soil affecting the depth response curve of the EMI measure and the resulting EC_a determination (Doolittle and Brevik, 2014; Cockx et al., 2009; Harvey and Morgan, 2009).

The small error relative to the values indicates greater model reliable (Table 3). In addition, the r and d indices, which indicates model precision and accuracy, respectively adds additional support to the model output reliability. Overall, the accuracy and precision of these developed models for atrazine transport parameters allow for further evaluation of how atrazine moves through the soil profile. Once, atrazine contamination impacts the environment moving through the soil toward the groundwater, moving in the surface water through runoff, or attached to a soil matrix; suitably calibrated EC_a survey data proves to be helpful for researchers in better understand atrazine movement on a given corn crop. This understanding can provide more accurate information for developing best management practices that aim to control atrazine's impact on the environment. BMP's such as the correct amount of atrazine to be applied in certain region of the field, at a certain moment of the crop growth, with a certain way of application are the ones to be improved using EMI and HYDRUS-2D coupled.

Generally, soils in this area are considered reasonably homogeneous loess silt loam. However, different characteristics can be noticed mainly in the southeast region of the field. Though these variations may be relatively small for soil classification, these differences impact atrazine transport. The southeast portion of the test site is located near a small drainage area. Because of that, the surface horizon in this area has been subject to some erosion and as a result the argillic horizon is located much closer to the surface. Therefore, sampling the 40 cm depth contains a greater clay content than other sampling locations. Fig. 3 shows high values for the EC_a at the southwest part of the map which agrees with the clay content presented in the Fig. 5A. Fig. 5B, 5C, and 5D show how atrazine movement parameters change according to this aspect of the area. The results presented in Fig. 5 and Table 3 clearly shows how the soil properties in the field could affect atrazine movement.

Based on the measure transport parameters, atrazine applied on the southwest part of the sample site would move through the soil profile much slower due to the greater near-surface clay content (Table 3). The interaction between atrazine and the clay in the soil matrix increases the retardation value (higher R), lowers the partition coefficient (low value of β) and increases the transfer coefficient (high value of ω). When the near-surface clay content is lower, it is expected the R value would be lower, the β value would be greater, and the ω would be lower. The binding of atrazine by the near-surface clay fraction would retain the atrazine in the upper layers of the soil profile. For surface water contamination, this would increase if the surface soil eroded to the receiving stream. For soils with little clay content, the risk would be greater for the atrazine to move through the profile potentially contaminating groundwater. It should be noted for this site, any atrazine that move through the profile would be bound in the argillic horizon below the surface soil. However, this data suggests the EMI sensor with response surface sampling could identify areas of a field susceptible to increased risk for surface or groundwater contamination.

Figs. 6 and 7 illustrates the challenge of trying to predict accurate transport of contaminants using average soil transport parameters in a model like HYDRUS-2D. The figure presents the relative errors for atrazine concentration comparing the average of the atrazine movement with the atrazine movement for each specific site of the sample site. Fig. 6E shows the relative errors are not as great for 20 cm depth in July when compared to Fig. 7E, which shows the relative errors for 20 cm depth in October. Fig. 6A, 6B, 7A, and 7B, specifically, indicate the parameters average does not predict atrazine movement well. Using the site-specific determined transport parameter provided a better prediction of how fast atrazine moves through the soil. However, Fig. 6F shows the relative errors for 40 cm depth in July indicating the parameters average provide good predictions. Therefore, it can be concluded that for a long term, even in a small area, the specific parameters for each site need to be considered once the average of parameters generally underestimates atrazine concentration at both depths and in both July and October.

Another point to be addressed is the differences in atrazine concentration at certain portions of the field. The atrazine decay in the northern portion of the field behaves differently in comparison with the atrazine decay in the southern portion, which is evidenced by Fig. 6C,D and Fig. 7C,D. In the northern portion, the atrazine concentration decays at 20 cm depth from July to October, while it increases at 40 cm depth in the same time frame, showing that with time passing, atrazine is accumulating in a deeper layer of the soil. In the southern portion, atrazine concentration increases in both 20 and 40 cm soil layers from July to October. That could be caused by different factors: first, the amount of clay existent in the southern portion of the field, which is evidenced by Fig. 5A, due to the presence of a argillic horizon exposed by erosion as explained before; second, the rain events in the months of July (76.2 mm), August (83.8 mm), and September (124.5 mm) that could contribute for washing the atrazine in the direction from the northern to the southern field portion; third, the possible preferential flow paths causing a lateral movement that were not evaluated by this research, which still could lead the atrazine to move faster in this

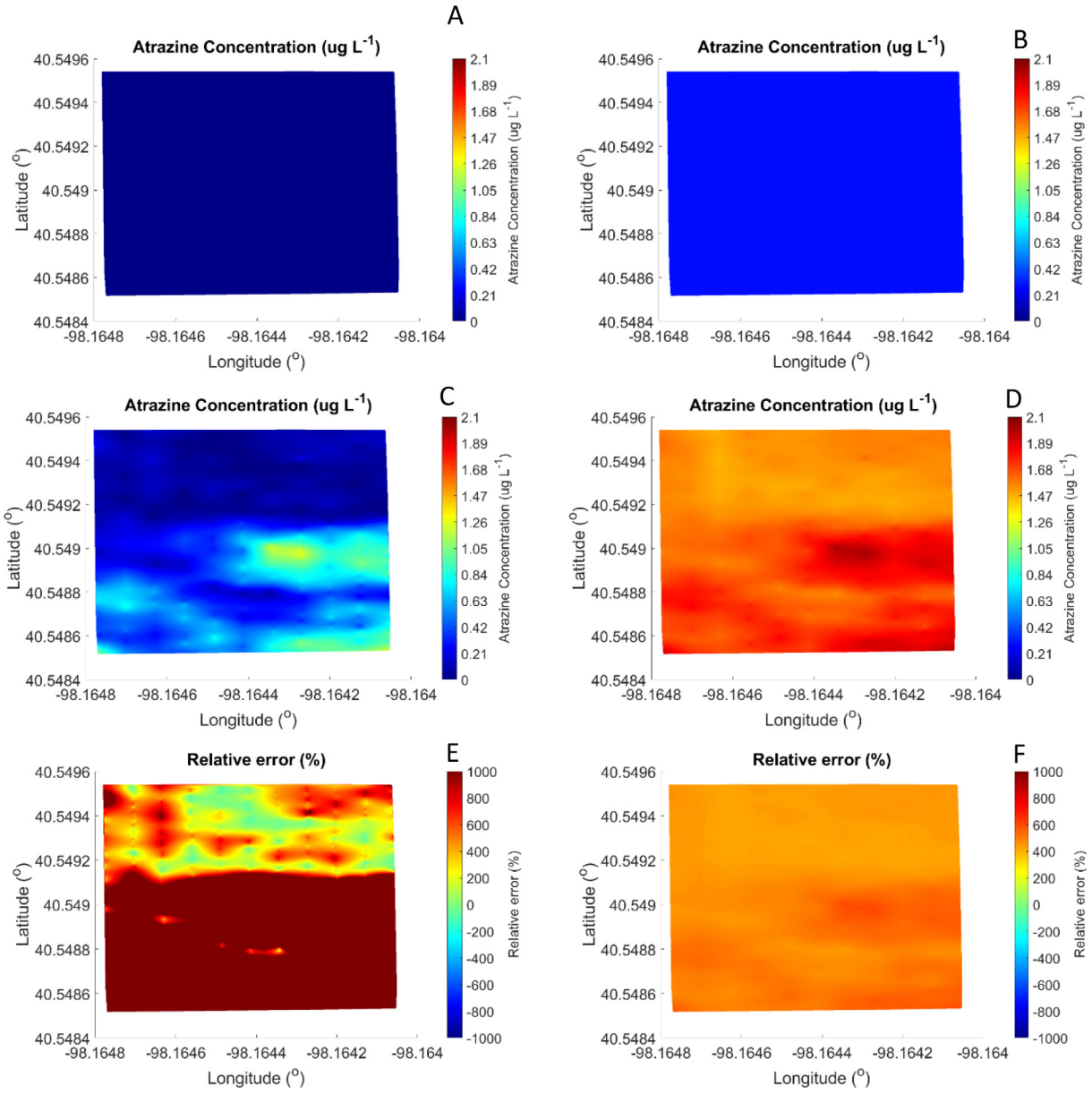

Fig. 6. (A) Average of atrazine concentration (μg L^{-1}) for July at 20 cm depth, (B) Average of atrazine concentration (μg L^{-1}) for July at 40 cm depth, (C) Site-specific atrazine concentration (μg L^{-1}) for July at 20 cm depth, (D) Site-specific atrazine concentration (μg L^{-1}) for July at 40 cm depth, (E) Relative error of atrazine concentration for July at 20 cm depth, and (F) Relative error of atrazine concentration for July at 40 cm depth. Scales of Fig. 6B and D differ from scale on Fig. 6A and C for better visualization.

direction; forth, the hydraulic conductivity that could be different in these regions of the field and enhance the lateral movement of water content carrying atrazine and interfere directly in the water infiltration.

5. Conclusions

This study evaluated whether EMI can be used to identify regions of a corn silage field for mitigating atrazine transport to groundwater. Within the results and statistical indices, there is potential of EMI technology for identifying areas subject to contamination of surface water. The correlations indicate a majority of EC_a response is driven by soil parameters that control the transport process, which leads to transport parameters being estimated from the EC_a. When using these parameters in HYDRUS 2D, the model predicts the spatially and temporal variable atrazine transport with high accuracy. Thus, HYDRUS-2D coupled with EC_a showed the regions of the field where atrazine concentration was being over and underestimated. Based on this, EMI as field scale tool showed promise for identifying critical regions of a field where atrazine transport can exceed expectations. Additional work will have to be done to determine the extensiveness of atrazine's leaching for these regions and whether atrazine should be prohibited or not. Using EMI sensor data combined with the HYDRUS-2D model provides valuable insight for developing of management practices to mitigate atrazine contamination of groundwater and more accurate information for decision makers to decide amount, season, and location of atrazine application. Additional studies expanding the use of HYDRUS 2D coupled with the EMI sensor data for other contaminants are planned.

Declaration of Competing Interest

The authors declare that they have no known competing financial interests or personal relationships that could have appeared to influence the work reported in this paper.

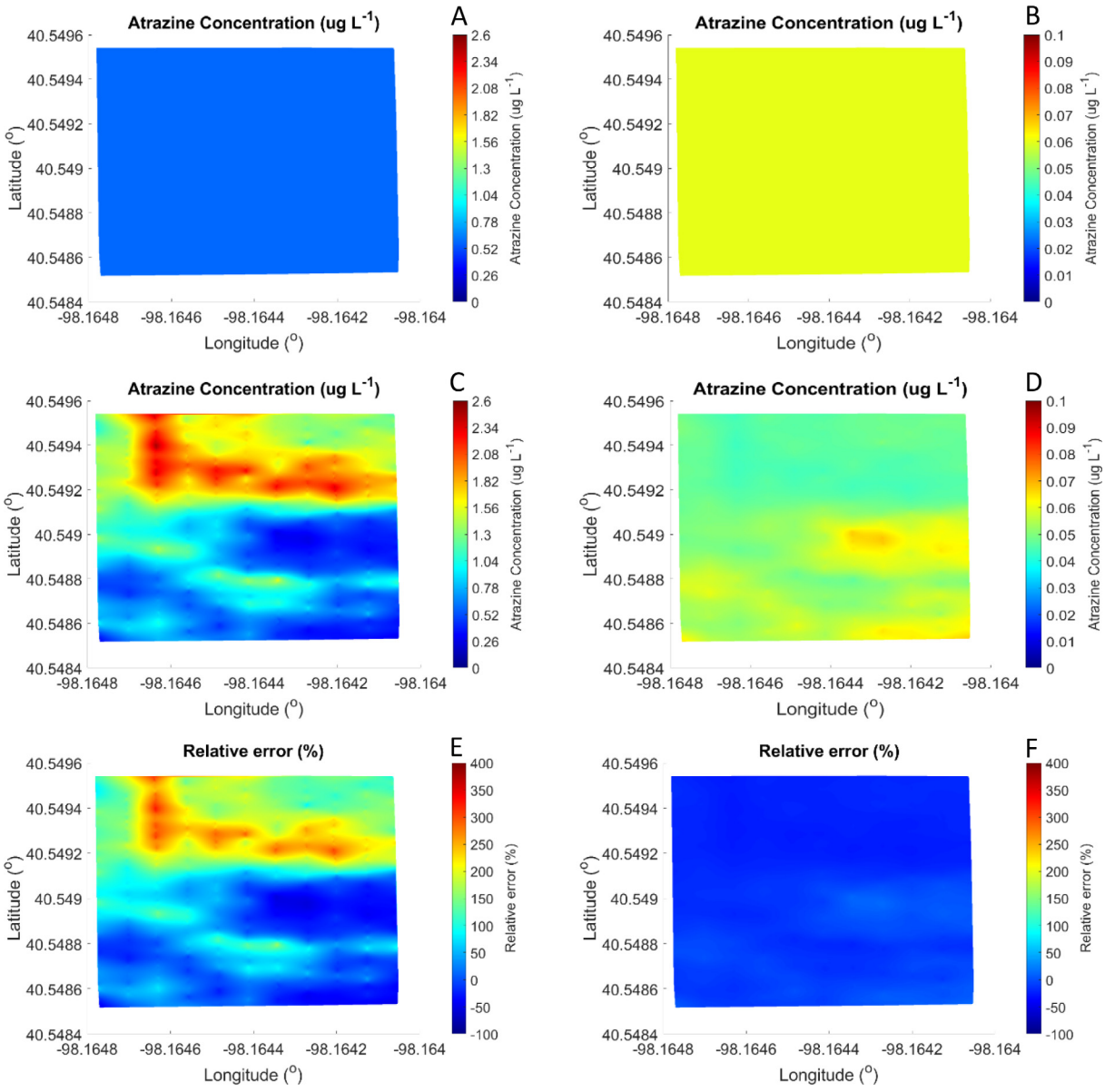

Fig. 7. (A) Average of atrazine concentration (μg L^{-1}) for October at 20 cm depth, (B) Average of atrazine concentration (μg L^{-1}) for October at 40 cm depth, (C) Site-specific atrazine concentration (μg L^{-1}) for October at 20 cm depth, (D) Site-specific atrazine concentration (μg L^{-1}) for October at 40 cm depth, (E) Relative error of atrazine concentration for October at 20 cm depth, and (F) Relative error of atrazine concentration for October at 40 cm depth.

Acknowledgment

This study was supported in part by the National Council for Scientific and Technological Development (CNPq) for granting scholarships to the first author and by the PQ grants.

The authors would like to thank the personnel from USMARC in Clay Center, the team of the Laboratory of Soil Physics of the Department of Biosystems Engineering, Luiz de Queiroz College of Agriculture (ESALQ/USP), the Editor and reviewers from Geoderma, and to the São Paulo Research Foundation (FAPESP) for the financial support (Proposals: #2017/07443-6, #2018/01915-6 and #2018/10164-4) and Meat Animal Research Center USMARC/USDA, Clay Center, NE, USA.

Mention of trade names or commercial products in this article is solely for the purpose of providing specific information and does not imply recommendation or endorsement by the USDA. USDA is an equal opportunity provider and employer.

References

Ackerman, F., 2007. The economics of atrazine. Int. J. Occup. Environ. Health 13, 441–449.

Al-Gaadi, K., 2012. Employing electromagnetic induction techniques for the assessment of soil compaction. Am. J. Agric. Biol. Sci. 4, 425–434.

Allen, R.G., Pereira, L.S., Raes, D., Smith, M. Crop evapotranspiration: Guidelines for computing crop water requirements. Rome: FAO, 1998. 300 p. (FAO – Irrigation and Drainage Paper,56).

Anlauf, R., Schefer, J., Kajitvichyanukul, P., 2018. Coupling HYDRUS-1D with ArcGIS to estimate pesticide accumulation and leaching risk on a regional basis. J. Environ. Manage. 217, 980–990.

Biradar, D.P., Rayburn, A.L., 1995. Chromossomal damage induced by herbicide contamination at concentrations observed in public water supplies. J. Environ. Quality, Madison 24, 1222–1225.

Bristow, K.L., Hopmans, J.W., Cote, C.M., Charlesworth, P.B., Thornburn, P.J., Cook, F.J., 2002. Development of improved water and nutrient management strategies through strategic modeling. In: Proc. 17th WCSS, pp. 14–21 Thailand.

Brogi, C., Huisman, J.A., Pätzold, S., von Hebel, C., Weihermüller, L., Kaufmann, M.S., van der Kruk, J., Vereecken, H., 2019. Large-scale soil mapping using multi-configuration EMI and supervised image classification. Geoderma 335, 133–148. https://doi.org/10.1016/j.geoderma.2018.08.001.

Cockx, L., van Meirvenne, M., Vitharana, U.W.A., Verbeke, L.P.C., Simpson, D., Saey, T.,

van Coille, F.M.B., 2009. Extracting topsoil information from EM38DD sensor data using neural network approach. Soil Sci. Soc. Am. J. 73 (6), 1–8.
Corwin, D.L., Lesch, S.M., 2005. Apparent soil electrical conductivity measurements in agriculture. Comput. Electron. Agric. 46, 11–44.
de Oliveira, L.A., Grecco, K.L., Tornisielo, V.L., Woodbury, B.L., 2019. Atrazine movement in corn cultivated soil using HYDRUS-2D: a comparison between real and simulated data. J. Environ. Manage. 248, 109311.
Doolittle, J.A., Brevik, E.C., 2014. The use of electromagnetic induction techniques in soil studies. Geoderma 223–225, 33–45.
Doolittle, J.A., Chibirka, J., Muniz, E., Shaw, R., 2013. Using EMI and P-XRF to characterize the magnetic properties and the concentration of metals in soils formed over different lithologies. Soil Horiz. 54 (3), 1–10. https://doi.org/10.2136/sh13-01-0009.
Dor, Maoz, Emmanuel, Simon, Brumfeld, Vlad, Levy, Guy J., Mishael, Yael G., 2019. Microstructural changes in soils induced by wetting and drying: Effects on atrazine mobility. Land Degrad Dev. 30, 746–755.
Eigenberg, R.A., Lesch, M.S., Woodbury, B.L., Nienaber, J.A., 2008. Geospatial methods for monitoring a vegetative treatment area receiving beef feedlot runoff. J. Environ. Qual. 37 S-68-S-77.
Feddes, R.A., Kowalik, P.J., Zaradny, H. Simulation of field water use and crop yield. In: Simulation Monograph, Pudoc, Wageningen, The Netherlands, pp. 9–30. 1978.
Fernandes, Ana Flavia Tonelli, Ping Wang, Christopher Staley, Jéssica Aparecida Silva Moretto, Lucas Miguel Altarugio, Sarah Chagas Campanharo, Eliana Guedes Stehling, and Michael Jay Sadowsky. “Impact of Atrazine Exposure on the Microbial Community Structure in a Brazilian Tropical Latosol Soil.” Microbes and Environments 35, no. 2 (2020): ME19143.
Friedmann, A. S. Atrazine inhibition of testosterone production in rat males following peripubertal exposure. Reproductive Toxicology, Limerick, v. 16, n.3, p. 275-279, May/June 2002.
Gärdeñas, A.I., Hopmans, J.W., Hanson, B.R., Šimůnek, J., 2005. Two-dimensional modeling of nitrate leaching for various fertirrigation scenarios under micro-irrigation. Agric. Water Manag. 74, 219–242.
Grecco, K.L., de Miranda, J.H., Silveira, L.K., van Genuchten, M.T., 2019. HYDRUS-2D simulations of water and potassium movement in drip irrigated tropical soil container cultivated with sugarcane. Agric. Water Manage. 221, 334–347.
Hanson, B.R., Šimůnek, J., Hopmans, J.W., 2008. Leaching with subsurface drip irrigation under saline, shallow-groundwater conditions. Vadose Zone J. 7 (2), 810–818.
Hansen, Samuel, P., Messer, Tiffany, L., Mittelstet, Aaron, R., 2019. Mitigating the risk of atrazine exposure: Identifying hot spots and hot times in surface waters across Nebraska, USA. J. Environ. Manage. 250, 11p.
Harvey, O.R., Morgan, C.L.S., 2009. Predicting regional-scale soil variability using single calibrated apparent soil electrical conductivity model. Soil Sci. Soc. Am. J. 73, 164–169.
Heil, K., Schmidhalter, U., 2012. Characterization of soil texture variability using apparent electrical conductivity at a highly variable site. Comput. Geosci. 39, 98–110.
Kandelous, M.M., Kamai, T., Vrugt, J.A., Šimůnek, J., Hanson, B.R., Hopmans, J.W., 2012. Evaluation of subsurface drip irrigation design and management parameters for alfafa. Agric. Water Manag. 109, 81–93.
Jaynes, D.B., Novak, J.M., Moorman, T.B., Cambardella, C.A., 1995. Estimating herbicide partition coefficients from electromagnetic induction measurements. J. Environ. Qual. 24, 36–41.
Kaufmann, M.S., von Hebel, C., Weihermüller, L., Baumecker, M., Döring, T., Schweitzer, K., Hobley, E., Bauke, S.L., Amelung, W., Vereecken, H., van der Kruk, J., 2020. Effect of fertilizers and irrigation on multi-configuration electromagnetic induction measurements. Soil Use Manag. 36, 104–116. https://doi.org/10.1111/sum.12530.
Kniss, A.R., 2017. Long-term trends in the intensity and relative toxicity of herbicide use. Nat. Commun. 8, 14865.
Lesch, S.M., Strauss, D.J., Rhoades, J.D., 1995a. Spatial prediction of soil salinity using electromagnetic induction techniques: 1. Statistical prediction models: a comparison of multiple linear regression and cokriging. Water Resour. Res. 31, 373–386.
Lesch, S.M., Strauss, D.J., Rhoades, J.D., 1995b. Spatial prediction of soil salinity using electromagnetic induction techniques: 2. An efficient spatial sampling algorithm suitable for multiple linear regression model identifi cation and estimation. Water Resour. Res. 31, 387–398.
Lesch, S.M., 2005. Sensor-directed response surface sampling designs for characterzing spatial variations in soil properties. Comput. Electron. Agric. 46, 153–180.
Lesch, S. M.; Rhoades, J.D.; Corwin, D. L. Esap-95 version 2.10R User Manual and Tutorial guide. Research Report 146. USDA-ARS George E. Brown, Jr Salinity Laboratory, Riverside, California. 2000.
Matteau, J.P., Gumiere, S.J., Gallichand, J., Létourneau, G., Khiari, L., Gasser, M.O., Michaud, A., 2019. Coupling of a nitrate production model with HYDRUS to predict nitrate leaching. Agric. Water Manage. 213, 616–626.
McBratney, A., Whelan, B., Ancev, T., 2005. Future directions of precision agriculture. Precision Agric. 6, 7–23.
Myers, R.H., 1986. Classical and Modern Regression with Applications. Duxbury Press, Boston.
Nalewaja J. D. Dissipation of atrazine residues In North Dakota Soils. Farm Research. Vol. 25, No. 3 (January - February, 1968).
Pittelkow, C.M., Liang, X., Linquist, B.A., van Groenigen, K.J., Lee, J., Lundy, M.E., van Gestel, N., Six, J., Venterea, R.T., van Kessel, C., 2015. Productivity limits and potentials of the principles of conservation agriculture. Nature 517, 365–368.
Prado, B., Duwig, C., Hidalgo, C., Müller, K., Mora, L., Raymundo, E., Etchevers, J.D., 2014. Transport, sorption and degradation of atrazine in two clay soils from Mexico: Andosol and Vertisol. Geoderma 232–234, 628–639.
Rhoades, J.D., F. Chanduvi, and S.M. Lesch. 1999. Soil salinity assessment: Methods and interpretation of electrical conductivity measurements. FAO Irrig. Drain. Pap. 57. FAO, Rome.
Rubira, R.J.G., Constantino, C.J.L., Otero, J.C., Sanchez-Cortes, S., 2020. Abiotic degradation of s-triazine pesticides analyzed by surface-enhanced Raman scattering. J. Raman Spectroscopy 51 (2), 264–273.
Saha, Ajoy, Bhaduri, Debarati, Pipariya, Ashvin, Ghosh, Rakesh Kumar, 2017. Linear and nonlinear sorption modelling for adsorption of atrazine onto activated peanut husk. Environ. Progress Sustainable Energy 36 (2), 348–358.
Sass, J.B., Colangelo, A., 2006. European Union bans atrazine, while the United States negotiates continued use. Int. J. Occup. Environ. health 12 (3), 260–267.
Shapiro, S.S., Wilk, M.B., 1965. An analysis of variance test for normality (complete samples). Biometrika 52, 591–611.
Sibson, R. A brief description of natural neighbor interpolation (Chapter 2). In V. Barnett. Interpolating Multivariate Data. Chichester: John Wiley. pp. 21–36. 1981.
Šimůnek, J., Hopmans, J.W., 2009. Modeling compensated root water and nutrient uptake.Ecological. Modeling 220 (4), 505–521.
Šimůnek, J., Šejna, M., van Genuchten, M.T., 1999. The HYDRUS-2D Software Package for Simulating the Two-dimensional Movement of Water, Heat, and Multiple Solutes in Variably-saturated Media. Version 2.0.
Šimůnek, J., Van Genuchten, M.T.H., Šejna, M., 2016. Development and applications of the HYDRUS and STANMOD softwares packages and related codes. Vadose Zone J. 7 (2), 587–600.
Sudduth, K., Kitchen, N.R., Chung, S.O., Drummond, S.T., 2010. Site-specific compaction, soil physical property, and crop yield relationships for claypan soils. Annual International Meeting of American Society of Agricultural and Biological Engineers. Paper no. 1009432. American Society of Agricultural and Biological Engineers, St. Joseph, Michigan.
TAIZ, L.; ZEIGER, E. MØLLER, I. M.; MURPHY, A. Plant Phyiology. 5. ed., Artmed. 918 p 2013.
Taylor, S.A., Ashcroft, G.M., 1972. Physical Edaphology. San Francisco, Freeman, pp. 533.
Tiefelsdorf, M., 2000. Modeling spatial processes: Th e identifi cation and analysis of spatial relationships in regression residuals by means of Moran’s I. Springer-Verlag, New York.
Toride, N.: Leij, F. J.; Van Genuchten, M. T. The CXTFIT code for estimating transport parameters from laboratory or field tracer experiments: Version 2.0. Research Report n.137, U.S Salinity Laboratory of Agricultural Research Service. USDA. Riverside, California, 1995, 121 p.
Triantafilis, J., Lesch, S.M., la Lau, K., Buchanan, S.M., 2009. Field level digital mapping of cation exchange capacity using electromagnetic induction and a hierarchical spatial regression model. Aust. J. Soil Res. 47, 651–663.
van Genuchten, M.T.H., 1980. A closed-form equation for predicting the hydraulic conductivity of unsaturated soils. Soil Sci. Soc. Am. J. 44, 892–898.
von Hebel, C., Matveeva, M., Verweij, E., Rademske, P., Kaufmann, M.S., Brogi, C., van der Kruk, J., 2018. Understanding soil and plant interaction by combining ground-based quantitative electromagnetic induction and airborne hyperspectral Data. Geophys. Res. Lett. 45 (15), 7571–7579.
Vrugt, J.A., Hopmans, J.W., Šimůnek, J., 2001a. Calibration of a two-dimensional root water uptake model. Soil Sci. Soc. Am. J. 65 (4), 1027–1037.
Vrugt, J.A., van Wijk, M.T., Hopmans, J.W., Šimůnek, J., 2001b. One-, two-, and three-dimensional root water uptake functions for transient modeling. Water Resour. Res. 37 (10), 2457–2470.
Wesseling, Z., Elbers, J.A., Kabat, P., van der Broek, B.J., 1991. SWATRE: Instructions for Input. Winand Staring Centre, Wageningen.
Wang, P.A.A.K., 2009. Sorption and desorption of atrazine and diuron onto water dispersible soil primary size fractions. Water Res. 43, 1448–1456. https://doi.org/10.1016/j.watres.2008.12.031.
Wang, M., Liu, H., Zak, D., Lennartz, B., 2020. Effect of anisotropy on solute transport in degraded fen peat Soils. Hydrol. Processes 34, 2128–2138.
Woodburry, B.L., Lesch, S.M., Eigenberg, R.A., Miller, D.N., Spiehs, M.J., 2009. Electromagnetic Induction sensor data to identify areas of manure accumulation on a feedlot surface. Soil Sci. Soc. Am. J. 73, 2068–2077.
Woodbury, B.L., Eigenberg, R.A., Varel, V., Lesch, S.M., Spiehs, M.J., 2011. Using electromagnetic induction technology to predict volatile fatty acid, source area differences. J. Environ. Qual. 40, 1416–1422.
Yale, R.L., Sapp, M., Sinclair, C.J., et al., 2017. Microbial changes linked to the accelerated degradation of the herbicide atrazine in a range of temperate soils. Environ. Sci. Pollut. Res. 24, 7359–7374. https://doi.org/10.1007/s11356-017-8377-y.
Yue, Lin, Ge, ChengJun, Feng, Dan, Huamei, Yu., Deng, Hui, Bomin, Fu., 2017. Adsorption–desorption behavior of atrazine on agricultural soils in China. J. Environ. Sci. 57, 180–189.